



# Prediction of Temperature Distribution of the Spindle System by Proposed Finite Volume and Element Method

V. Prabhu Raja<sup>1</sup> · R. Sathiya Moorthy<sup>2</sup>

Received: 9 April 2018 / Accepted: 29 January 2019 / Published online: 8 February 2019  
© King Fahd University of Petroleum & Minerals 2019

## Abstract

High-speed machining is one of the emerging cutting processes possessing tremendous potential in the arena of increased metal removal rates as well in achieving improved surface finish, burr-free edges, dimensional accuracy and a virtually stress-free component after machining. However, as known the performance of a machine tool depends on a number of factors of which the most important is the thermal behavior of the high-speed spindle. Thus, the temperature rise and the displacement due to temperature variation in the spindle components will severely affect the thermal characteristics of high-speed motorized spindle. Hence, it is significant to study its thermal behavior, and so in this paper, a coupled fluid–thermal (CFT) of a high-speed spindle is developed to simulate fluid-structural conjugate heat transfer. Based on the proposed model, the thermal characteristic of the high-speed spindle system is studied. The investigation revealed that the proposed CFT analysis for the motor cooling path has shown a minimum deviation in spindle temperature approximating to 7.6% when compared with that of attained experimental results at high speed.

**Keywords** High-speed spindle · Thermal characteristics · Cooling channel · Convection coefficient · Coupled fluid–thermal analysis

## 1 Introduction

The spindle assembly is one of the most important parts in a machine tool. Machine tools today are operated at very high speed which increases its amplitude of vibration and heat generation, imposing serious limitations on accuracy and productivity of the machine tool. Many researches are going on related to the design of spindle assembly, and there is a strong need to accurately predict the thermal characteristics of the machine tool spindle for an efficient design of cooling system. This is particularly true for high-speed and special purpose spindle assemblies. The majority of high-speed machine tools employ spindles with hybrid rolling element bearings. The higher operating speed of spindle generates enormous heat in the spindle system which has a significant influence on the working capability and machining

accuracy [1]. Zeljovik and Gatalo [2] developed a methodology to study the static and dynamic behavior of high-speed machine tool spindle in different thermal conditions, with different bearing arrangements. The obtained experimental results were compared with computer-aided analysis results which were done using different software (I-DEAS, ALGOR, SAP- 90 and VRETENO). The results obtained using VRETENO software had better agreement with the experimental results since it uses Timoshenko beam theory which considers the influence of transverse shear vibrations. The authors concluded that even at the design phase the relevant characteristics of the designed spindle assembly cannot be obtained. Lack of understanding about the concept of thermal effects in the spindle limits its reliability. To characterize the heat transfer of a high-speed motorized spindle, a finite difference thermal model was developed and verified by a high-speed motorized milling spindle of 32 KW with maximum speed of 25,000 rpm [3]. The developed model was validated against experiment for steady state, transient state and power balance analysis. Steady-state validation included 14 selected element locations at five different speeds, while for the transient-state validation two typical temperature histories of the bearing and at the spindle nose were presented.

✉ R. Sathiya Moorthy  
rsathiyamoorthy@gmail.com

<sup>1</sup> Department Mechanical Engineering, PSG College of Technology, Coimbatore, India

<sup>2</sup> Department Mechanical Engineering, Anna University Regional Campus, Coimbatore, India



The result of the model agreed with the experimental result despite the low number of shafts.

Bossmanns and Tu [4] developed a power flow model to demonstrate the heat generated in high-speed motorized spindle by built in motor and bearing under the influence of speed and preload. The influence of cooling system and lubrication system on the temperature field of a high-speed motorized spindle was studied using a finite element model [5]. The developed model was tested under different working conditions and compared with test model. The predicting error was 3.6% when the spindle speed was 15,000 rpm. Ma et al. [6,7] studied the effect of lubrication in the spindle. They proposed some solution to the lubrication problem. If the spindle is not high, grease lubrication shall be used directly instead of oil–gas lubrication system [6]. A better efficiency of heat transfer was obtained with oil–air lubrication than oil–water lubrication [7].

Sheng et al. [8] developed a finite element model of the spindle and used ANSYS to analyze the steady-state temperature field of the spindle. They proposed installing a sleeve in front of the spindle box would reduce the thermal error of the machine tool spindle. While studying the thermal performance of the high-speed spindle by finite element analysis and experiments, Wen and Wang [9] identified the maximum temperature rise was at the area of electromotor followed by rolling bearing. The temperature rise gives rise to thermal expansion of the spindles in the radial direction [10]. To reduce the temperature rise reciprocating cooling channels shall be preferred than single and double helical cooling channels [10]. Flow of cooling oil, structure of the cooling system and the use of low power loss of motor will improve the thermal characteristics of the high-speed spindle [11].

Cui et al. [12] proposed a three-dimensional finite element method to calculate the thermal deformation by considering the thermal contact resistance. In particular they take into account the appropriate parameters of the machine tool joints and structural linkages in the prediction of the thermal contact resistance. Liu et al. [13] carried out the thermo-mechanical coupled dynamic analysis for high-speed motorized spindles, and the damp of the system is obtained by using the modal analysis. Zeji and Ding [14] designed a thermal error control system for a motorized spindle based on the thermal deformation balance principle. They used carbon fiber-reinforced plastic to restrain the thermal elongation of the metal spindle housing. Zhang et al. [15] proposed a finite element method and parametric optimization (Levenberg–Marquardt method) approach to predict the thermal error of a motorized high-speed spindle.

Most of the previously published studies have revealed that the temperature of the working fluid is assumed to be a constant; in other words, the heat transfer between solids and working fluid in a spindle is infinite; however, in real cases it is not so. In order to bring more exactness in the prediction of

temperature distribution of the high-speed spindle, this paper proposed a coupled fluid volume and finite element method is carried out. The thermal analysis of high-speed spindle is simulated by considering two different cases. In the first case, the heat transfer coefficient in the cooling path [4] is estimated based on the empirical relations and it was set to constant at  $2.11 \times 10^{-4} \text{ W/mm}^2\text{C}$ , similar to the analysis done in [5–11,15,16] using 2D axi-symmetric models. In the second case, the heat transfer coefficients are obtained using CFD software based on the flow rates of the coolant inside the path.

## 2 Heat Generation in the Motor

The electrical motor of a motorized spindle is a significant source of heat. Motorized spindles typically use AC induction motors, and the effective input power of the motor is given by Eq. (1),

$$P = \sqrt{3} \cdot U \cdot I \cdot \cos \varphi \quad (1)$$

where ‘ $U$ ’ is input voltage and ‘ $I$ ’ is the current through each lead. The phase angle ‘ $\varphi$ ’ between voltage and current determines the relative amount of effective power versus the measured apparent power. The effective electric input power is converted into mechanical output power and losses. The major portion of the losses is converted into heat.

The motor heat generation is estimated with the knowledge of speed and torque and is given by Eq. (2)

$$Q_{\text{motor}} = 2 \times \Pi \times f_{\text{motor}} \times T_{\text{motor}} \times \left( \frac{1 - \eta_{\text{motor}}}{\eta_{\text{motor}}} \right) \quad (2)$$

where the  $f_{\text{motor}}$  is the motor frequency, while torque  $T_{\text{motor}}$  is determined from the sum of torques related to actual bearing friction, windage losses, the cutting forces and acceleration, and  $\eta_{\text{motor}}$  is the motor efficiency.

## 3 Modeling of the Spindle System

The geometric model of KaVo EWL spindle which uses EV70-70.2 high-speed motor with specifications: power 4.7 kW, speed 40,000 rpm, frequency 750 Hz, no. of poles 2, has been considered for analysis. The spindle is assembled with a pair of GMN make (SM6005) angular contact ceramic ball bearings at the front side and pair of SNFA make (VEX 17) angular contact ceramic ball bearings at the rear side. A 3D model of the above spindle was developed using Pro/Engineer software, and its sectional view is shown in Fig. 1.

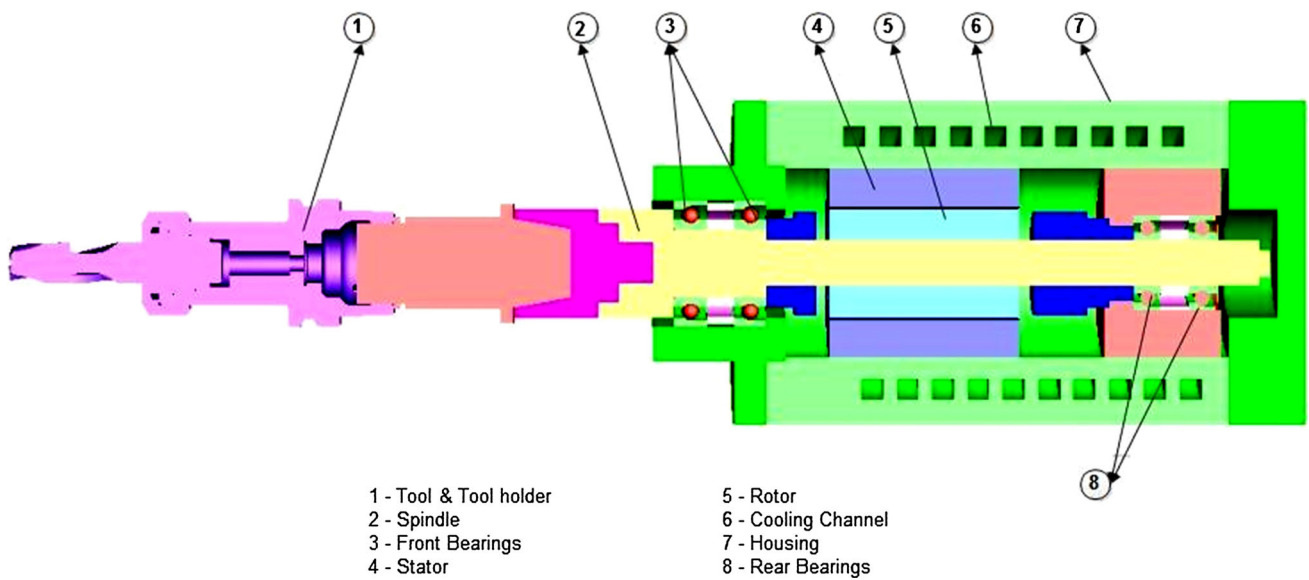


Fig. 1 Details of the high-speed spindle unit

### 4 Temperature Distribution with Constant Convection Coefficient

The finite element model of the high-speed spindle under consideration is developed using ANSYS software. The ‘meshing’ module of ANSYS generates the mesh structure for the spindle with high precision as shown in Fig. 2 and ensures better mesh shapes which is of high quality. An analysis of the meshing module output of the spindle reveals that the meshes are composed of tetrahedral and hexahedral elements. Prior to computation, a thorough verification of the mesh convergence of the numerical solution was performed in order to ensure the accuracy and validity of the numerical results.

A convergence test was performed on the finite element model so as to ensure the developed model accuracy. Fineness of the mesh was gradually increased by choosing the maximum edge length of the element in the range three to one, and analysis was carried out on each of the resulting models. It is observed that the temperature values are nearly the same for

fineness from two to one. It follows that a further increase in fineness of mesh will not help to improve the accuracy of the results but will lead to higher memory requirements. Hence, in the present work, the spindle assembly is discretized using a fineness value of two and the corresponding number of elements is 338,862.

The heat generated at the tool–workpiece interface is removed by the cutting fluid. Therefore, the heat generated by the spindle bearings and spindle motor are the dominant heat sources causing thermal deformation. The heat dissipation is governed by the forced convective heat transfer of coolant in coolant channel and the flow of air around the spindle.

The convection coefficient is estimated based on the equation done by Raja [16], and it is found to be a constant value.

$$\left. \begin{aligned} h &= Nu \cdot k / D_h \\ Nu &= 0.023 Re^{0.8} Pr^{0.3} \\ Re &= (V \cdot D_h) / \gamma \end{aligned} \right\} \quad (3)$$

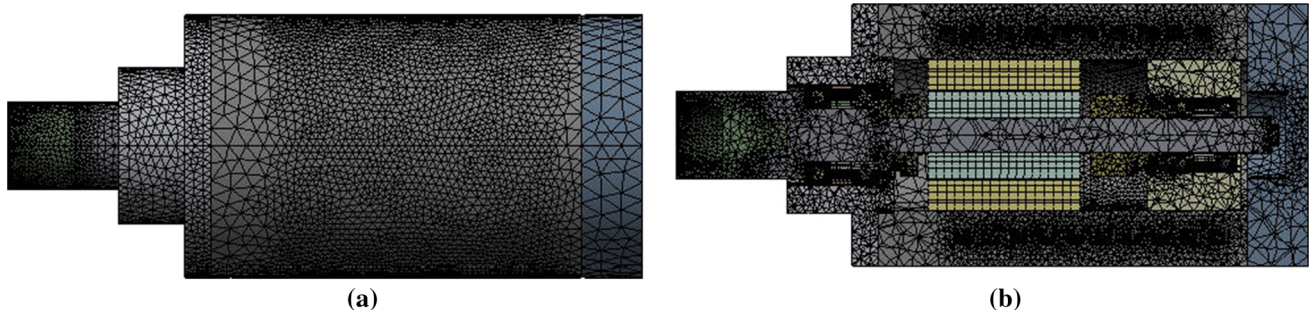


Fig. 2 Spindle a meshed model, b interior mesh

**Table 1** Heat generation value for thermal analysis [16]

Description	15,000 rpm	40,000 rpm
Front bearing heat generation/ball (W)	2.5	55
Rear bearing heat generation/ball (W)	1	14
Stator heat generation (W)	84	220
Rotor heat generation (W)	220	420

where  $Nu$  is Nusselt number,  $Re$  is Reynolds number (greater than 10,000) based on diameter, and  $Pr$  is Prandtl number ( $0.7 < Pr < 100$ ) of the coolant,  $D_h$  is hydraulic diameter,  $\gamma$  is the kinematic viscosity of the fluid, and  $k$  is the thermal conductivity of the fluid.

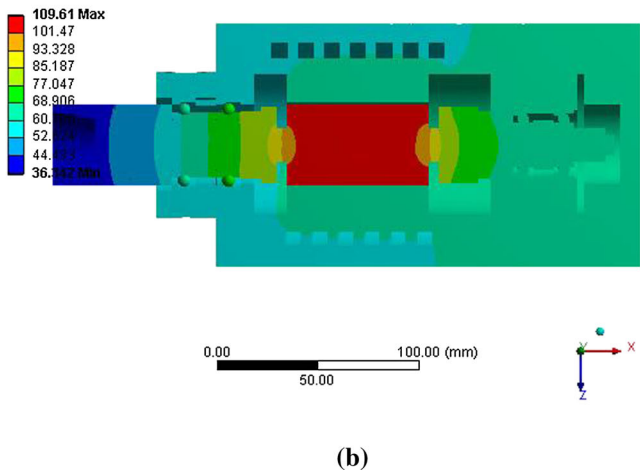
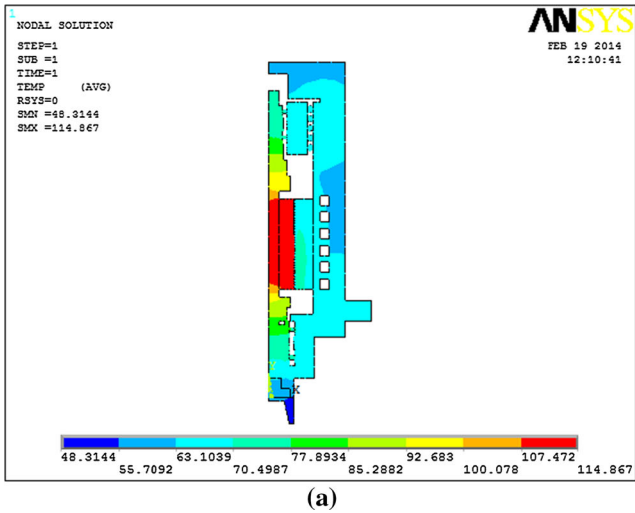
The heat transfer coefficient applied in the bearing and housing is  $227 \times 10^{-6} \text{ W/mm}^2\text{C}$  and  $10 \times 10^{-6} \text{ W/mm}^2\text{C}$ , respectively, while the heat transfer coefficient applied in the stator–rotor gap is  $295 \times 10^{-6} \text{ W/mm}^2\text{C}$ .

The analysis is carried out in the free spinning condition at spindle speeds of 15,000 rpm and 40,000rpm and with the input parameters [16] as shown in Table 1.

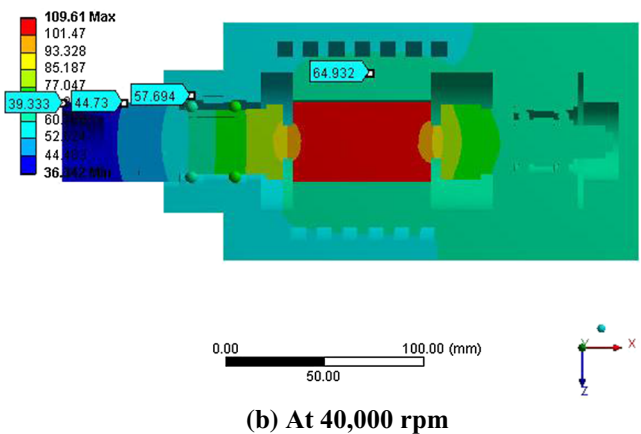
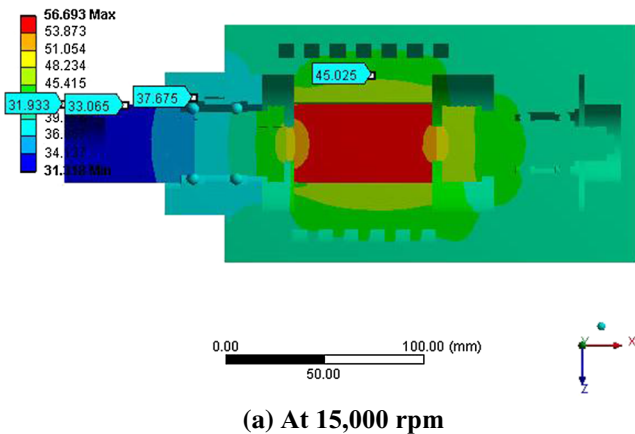
Figure 3a, b shows a comparison of the temperature distribution at 40,000 rpm obtained using 2D and 3D models. Notice that the maximum temperature is attained at the rotor and is found to be 114.86°C based on 2D model, while the proposed 3D model predicts the maximum temperature of rotor to be 109.61°C, considering constant heat transfer coefficient of the coolant.

Figure 4a, b shows a comparison of temperature distribution of spindle system obtained using constant convection coefficient in the 3D model by FEM. It is seen from Fig. 4a, b the stator temperature is 45°C and 65°C at 15000 rpm and 40,000 rpm, respectively. The corresponding temperature of the front bearing outer race increases from 37.5°C to 57.5°C.

Figures 3a and 4b show the front bearing outer race temperature as 68.6°C and 57.5°C, at 40,000 rpm speed in 2D



**Fig. 3** a: Temperature distribution in °C at 40,000 rpm using 2D model [16]. b: Temperature distribution in °C at 40,000 rpm using 3D model



**Fig. 4** Temperature distribution in °C with constant convection coefficient



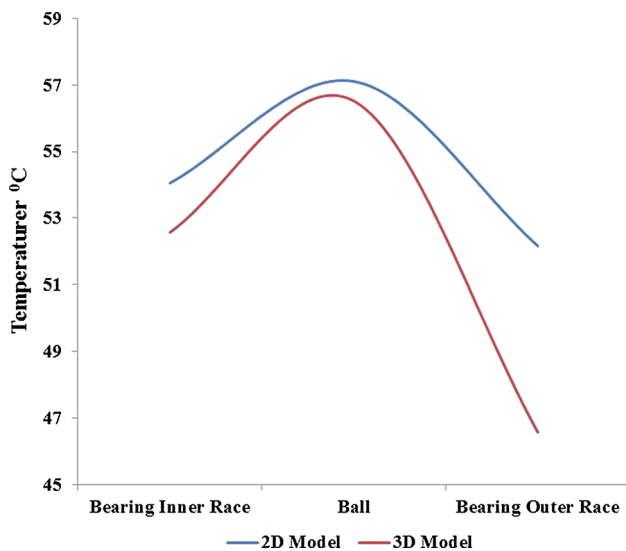


Fig. 5 Bearing temperature distribution at 40,000 rpm

and 3D model. The difference in temperature is due to the assumptions made in 2D FEM, where the balls are assumed as ring, which has line contact, whereas in reality there is a point contact between the balls and raceways and it has been incorporated in 3D models. In order to ascertain the above effect, the temperature distribution of the spindle was determined by without considering the coolant flow, stator heat generation and rotor heat generation. The temperature predicted in the inner raceway, ball and outer raceway of front bearing is shown in Fig. 5. It is evident that the outer raceway temperature predicted by the 3D model is lesser and realistic in magnitude due to the fact that the resistances to heat flow are higher, due to point contact between the balls and raceways.

### 5 Results and Discussion

The temperature distribution of the high-speed spindle is predicted through coupled fluid thermal analysis by finite volume and element method (FVEM). An estimate for energy is obtained incorporating the pressure of fluid using RNG k-epsilon turbulence model and is shown in Eqs. (4) and (5). The convergence criterion for energy (4) and (5) is obtained when the residuals of all the variables are less than  $1.0 \times 10^{-4}$ ,

$$\frac{\partial}{\partial t}(\rho E) + \frac{\partial}{\partial x_i}[u_i(\rho E + p)] = \frac{\partial}{\partial x_j} \left( k_{\text{eff}} \frac{\partial T}{\partial x_i} + u_i(\tau_{ij})_{\text{eff}} \right) + S_h \tag{4}$$

where  $E$  is the total energy,  $k_{\text{eff}}$  is the effective thermal conductivity, and  $(\tau_{ij})_{\text{eff}}$  is the deviatoric stress tensor and it represents viscous heating, defined as

$$(\tau_{ij})_{\text{eff}} = \mu_{\text{eff}} \left( \frac{\partial u_j}{\partial x_i} + \frac{\partial u_i}{\partial x_j} \right) - \frac{2}{3} \mu_{\text{eff}} \frac{\partial u_k}{\partial x_k} \delta_{ij} \tag{5}$$

The source of heat taken for the analysis is the stator heat generation. HYPSPIN VG5 synthetic oil whose density is  $840 \text{ kg/m}^3$  and thermal conductivity to be  $0.6 \text{ W/m}^\circ\text{C}$  is used as coolant.

The contours of temperature ( $^\circ\text{C}$ ) and velocity (m/s) are shown in Fig. 6a, b, respectively. The predicted outlet temperature of the coolant is found to be  $32.9^\circ\text{C}$  and  $30^\circ\text{C}$  when the velocity is varied from 0.9 to 4.3 L/min which corresponds to a Reynolds number of 2000 and 6000, respectively. The flow velocity of 4.3 L/min has better heat extraction, and further

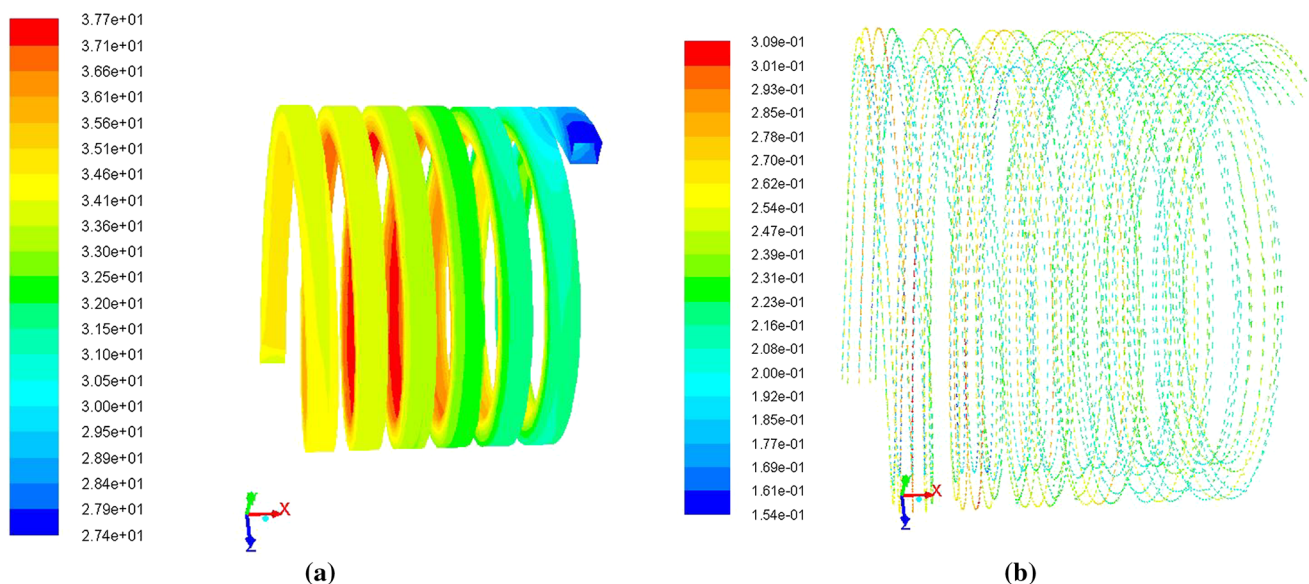
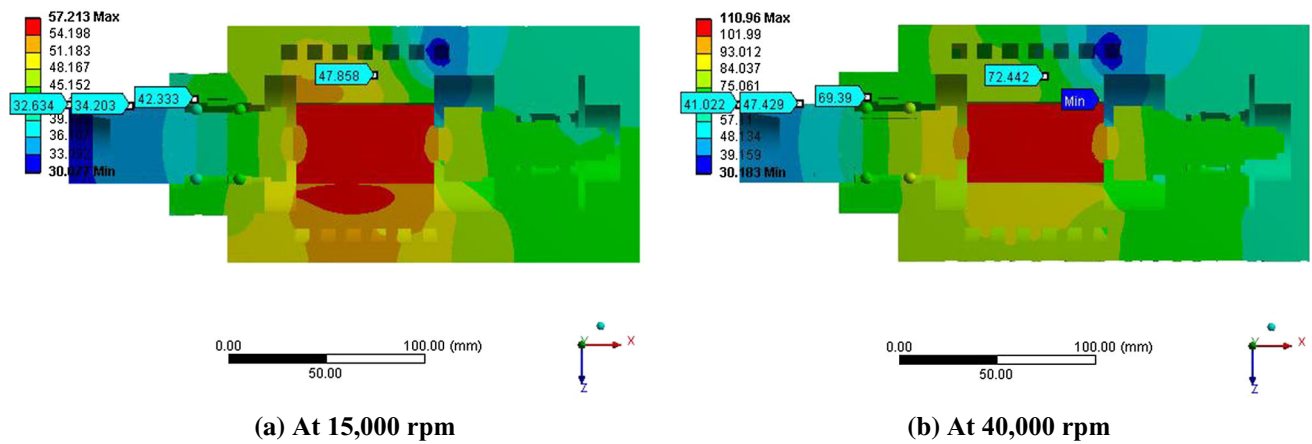


Fig. 6 a: Temperature contour of the cooling path. b: Velocity vector of the cooling path



**Fig. 7** Temperature distribution in °C with varying convection coefficient

**Table 2** Experimental and numerical estimates of temperature for 4.7 kW, 40,000 rpm spindle with 1.7L/min flow rate

Location	Speed (rpm)	Experiment [16] (°C)	2D with constant h [16] (°C)	% Deviation	3D with constant h (°C)	% Deviation	3D with varying h (°C)	% Deviation
Stator temperature	15,000	41.3	48.1	16.46	45.29	9.66	48.51	17.46
	40,000	72.5	68.1	6.07	64.99	10.36	73.28	1.08
Front bearing outer race	15,000	39.7	45.3	14.11	37.61	5.26	42.30	6.55
	40,000	65.0	68.6	5.54	57.47	11.58	69.10	6.31
Spindle nose	15,000	38.4	42.2	9.90	32.91	14.30	34.00	11.46
	40,000	51.2	55.0	7.42	44.61	12.87	48.14	5.98
Tool holder tip	15,000	35.3	40.4	14.45	31.93	9.55	32.65	7.51
	40,000	44.4	48.4	9.01	39.30	11.49	41.02	7.61

increase in the flow velocity does not have any significant increase in the heat extraction rate. So the flow velocity is fixed as 4.3 L/min for the forthcoming comparison.

The inlet and outlet of the coolant channel are placed closer to the rear bearings and front bearings, respectively, since the temperature of the coolant increases along the coolant path by 10 °C as shown in Fig. 6a. The convection coefficient of the coolant is expected to reduce from inlet to outlet. The effect of the above variation is seen by a corresponding deviation in temperature distribution in the proximity of the coolant path from Fig. 7a, b. The temperature variation from inlet to outlet is found to be 41.7–49.6 °C and 59.1–80.1 °C for 15,000 rpm and 40,000 rpm, respectively. On the other hand there is no significant variation in temperature distribution closer to the coolant path, when constant convection coefficient is applied as shown in Fig. 4a, b.

Experimental results stated by Raja [16] on a 3-axis machining center fitted with 4.7 kW, 40,000 rpm spindle unit along with a drive unit and chiller unit has been used for comparison. The experimental and numerical estimates of temperature at the stator, outer race of the front bearing, spindle nose and tool holder tip are shown in Table 2.

It is seen from Table 2 that at high speed (i.e., 40,000 rpm), it is observed that the maximum difference between the experimental and numerical results by the proposed 3D varying h method is 7.61% (by considering values in different locations). It is also noticed that the temperature deviation values using the proposed method are less when compared with Raja [16] estimation, except for the front bearing outer race, and the absolute difference in temperature is 0.5 °C only. However, the 3D model with constant convection coefficient by FEM yields higher temperature deviation, when compared with that of Raja [16] 2D model estimated at higher speed. The deviation in temperature is less for the proposed method when compared with the 2D model and 3D model with constant convection coefficient. This is due to the fact that the varying convection coefficient as predicted through coupled field analysis by FVEM leads to a more realistic simulation of the heat extracted by the coolant along the fluid path. This validates the suitability of proposed methodology for predicting temperature distribution in 3D models.

## 6 Conclusion

In this paper, the FEM model of the motorized high-speed spindle is set up, to explore on the temperature distribution which includes the effect of the cooling path. The fluid–thermal coupled module predicts fare better results when compared with constant convection coefficient thermal analysis. Simulation results reveal that the deviation in the temperature distribution in the spindle has been significantly reduced by coupling the exact cooling fluid in simulation. The results prove the reliability of coupling CFD in thermal analysis which can provide reference for design of high-speed spindle system. This suggests that the use of exact parameters of convection coefficient of the coolant in simulation gives more accurate results compared to values calculated by the empirical relations for coolant parameters.

## References

- Segida, A.P.: Calculation of the temperature field and thermal distortions of spindle assemblies and boxes. *Sov. Eng. Res.* **4**, 72–74 (1984)
- Zeljko, M.; Gatalo, R.: Experimental and computer aided analysis of high-speed spindle assembly behaviour. *Ann. CIRP* **48**, 325–328 (1999)
- Bossmann, B.; Tu, J.F.: A thermal model for high speed motorized spindles. *Int. J. Mach. Tools Manuf.* **39**, 1345–1366 (1999)
- Bossmann, B.; Tu, J.F.: A power flow model for high speed motorized spindles-heat generation characterization. *ASME J. Manuf. Sci. Eng.* **123**, 494–505 (2001)
- Zhang, L.; Li, C.; Wu, Y.; Zhang, K.; Shi, Huaitao: Hybrid prediction model of the temperature field of a motorized spindle. *Appl. Sci.* **7**, 1091–1104 (2017)
- Ma, P.; Zhou, B.; Li, Haipeng: Finite element analysis on thermal characteristics of lathe motorized spindle. *Adv. Mater. Res.* **311**, 2434–2439 (2011)
- Ma, P.; Zhou, B.; Li, D.N.; Xiao, S.H.; Wang, C.Y.: Thermal analysis of high speed built-in spindle by finite element method. *Adv. Mater. Res.* **188**, 596–601 (2011)
- Sheng, Z.; Zhu, Z.; Liu, C.; Zhang, C.: Research on thermal characteristic of spindle system of CNC machine tool. *Adv. Mater. Res.* **510**, 23–27 (2012)
- Wen, H.X.; Wang, M.Y.: Thermal characteristics finite element analysis and temperature rise experiment for high speed motorized spindle. *Appl. Mech. Mater.* **52**, 1206–1211 (2011)
- Huang, Y.-H.; Huang, C.-W.; Chou, Y.-D.; Ho, C.-C.; Lee, Ming-Tsang: An experimental and numerical study of the thermal issues of a high-speed built-in motor spindle. *Smart Sci.* **4**, 160–166 (2016)
- Liu, Z.; Chu, Z.; Cheng, Q.; Liud, G.: Thermal performance analysis for high-speed spindle of horizontal machining center. *Adv. Mater. Res.* **179**, 298–303 (2011)
- Cui, Y.; Li, H.; Li, T.; Chen, L.: An accurate thermal performance modeling and simulation method for motorized spindle of machine tool based on thermal contact resistance analysis. *Int. J. Adv. Manuf. Technol.* (2018). <https://doi.org/10.1007/s00170-018-1593-x>
- Liu, J.; Zhang, P.: Thermo-mechanical behavior analysis of motorized spindle based on a coupled model. *Adv. Mech. Eng.* **10**, 1–12 (2018)
- Zeji, G.E.; Ding, X.: Design of thermal error control system for high-speed motorized spindle based on thermal contraction of CFRP. *Int. J. Mach. Tool Manuf.* **125**, 99–111 (2018)
- Zhang, L.; Li, J.; Wu, Y.; Zhang, K.; Wang, Y.: Prediction model and experimental validation for the thermal deformation of motorized spindle. *Heat Mass Transf.* (2018). <https://doi.org/10.1007/s00231-018-2317-3>
- Raja, V.P.: Study on thermal behavior of motorized high speed spindles. Ph.D dissertation. Bharathiar University. India (2004)

